NETWORK RECOVERY FROM UNIAXIAL EXTENSION: I. ELASTIC EQUILIBRIUM*

C. M. ROLAND

NAVAL RESEARCH LABORATORY, CHEMISTRY DIVISION, CODE 6120, WASHINGTON, D.C. 20375-5000

INTRODUCTION

The relationship between the structure of a polymeric network and its response to mechanical perturbation is of interest, not only from obvious practical considerations, but for the insights thereby provided into the physics of long chain molecules. The stresses during the retraction of a stretched rubber are usually lower than the corresponding extensional stresses[1]. The primary reason for this strain softening is the retarded response of network chains due to the viscous drag exerted by neighboring chain segments. Such viscoelastic hysteresis is of course only observed if a state of mechanical equilibrium is not maintained during the deformation. Recently it has been reported that the mechanical behavior of a deformed network in the process of returning to the unstrained state is accurately described by equilibrium models of affinely deforming elastic chains[2]. The remarkable nature of this claim is amplified by ensuing reports that the crosslink density dependence of the nonequilibrium stress during retraction, as well as its strain dependence, is quantitatively in accord with the predictions of simple rubber elasticity theory[3–5], and that the modulus measured for rubbery solids after a uniaxial extension cycle is equal to within an additive constant to that given by the statistical theory for affine networks[6]. Notwithstanding this accumulating evidence, there are obvious difficulties with suggestions that the viscoelastic motion of junctions might be accurately described by equilibrium network models. This report relates recent efforts to probe the relationship between the elastic behavior of a network and its recovery from extensional deformation.

BACKGROUND

Determination of the equilibrium stress developed upon straining is the starting point for any attempt to account for the general deformation behavior of a crosslinked polymer. A sufficiently long (*ca.* 100 backbone bonds) free flexible chain will exhibit a statistical end-to-end separation described by a Gaussian distribution function. The nature of the intermolecular interactions does not modify this Gaussian behavior as long as such interactions are independent of chain configuration. The force required to distend the chain is directly proportional to the displacement, at least when the resulting end-to-end distance does

* Received September 20, 1988; revised May 8, 1989. B.

not approach the contour length of the chain. The problem of deducing the stress–strain relationship for a collection of chains attached to one another entails determination of the response of a given chain to the imposition of a bulk deformation. The crosslink sites in a real network are embedded in a high concentration of neighboring chain segments. At typical crosslink densities, spatially neighboring junctions are not topological neighbors; that is, the volume existing between a directly connected pair of junctions will contain many other junctions. Such interpenetration of network crosslink points is suggestive of an affine response to mechanical perturbations, whereby the network deforms not as a collection of individual chains, but rather as a continuum in which the crosslink points are embedded. The composition of junctions neighboring a given junction remains unchanged during an affine deformation; consequently, displacement of the chain junctions from their instantaneous end-to-end separation in a state of ease will be proportional to the macroscopic displacement of the specimen. For an affine network, the stress, defined as the ratio of the retractive force to the undeformed cross-sectional area (of the dry state for networks containing diluent) is given by[7,8]

$$\sigma_{aff} = NkTv^{-1/3}v_x^{2/3}f(\lambda) \tag{1}$$

with

$$f(\lambda) = \lambda - \lambda^{-2}, \tag{2}$$

where λ is the ratio of the final, l, and initial, l_0, specimen lengths, N denotes the density of elastically effective network chains in the dry rubber, and kT has its usual significance. The factor $v_x^{2/3}$ accounts for the compression of the network chains when crosslinked at a volume fraction v_x and subsequently deformed in the dry state[9]. The factor $v^{-1/3}$, where v is the volume fraction of network chains in the sample during deformation, accounts for the effect of swelling on the configurational entropy of the network and on the number of network chains per cross-sectional area. Even in the limit $v = 1$, the concept of junctions as firmly embedded as required by the affine model is inconsistent with the large free volume available to chain segments in the elastomeric state and the thermal agitation they experience. An alternative approach to rubber elasticity theory embodies the concept of volumeless chains able to freely pass through one another. Although the average displacement of such phantom network strands would be proportional to the macroscopic strain, Brownian motion of the junctions would enable their diffusion significant distances from an end-to-end separation characterized by affine displacement. The elastic stress for a perfect (no dangling ends) network of phantom chains is[7,10]

$$\sigma_{phan} = (1 - 2/\phi)NkTv^{-1/3}v_x^{2/3}f(\lambda), \tag{3}$$

where ϕ is the junction functionality (and $2N/\phi$ is the crosslink density). The greater freedom to rearrange configurations enjoyed by a phantom network reduces the displacement of chains in response to a macroscopic deformation and thus reduces the equilibrium stress (by half for tetrafunctional crosslinks) from that of affinely deformed junctions.

Real networks exhibit a strain dependence of their elastic stress that is at

variance with the predictions of either the affine or the phantom network models. This is not unexpected, since the junctions in a real polymer network can, by virtue of their thermal energy, fluctuate away from positions corresponding to affine displacement, while interferences from neighboring chains reduce the magnitude of such fluctuations from that available to a phantom network.

For uniaxial extension over broad ranges of strain, a semiempirical approach to the strain dependence of the elastic modulus enjoys wide application. The strain energy of an incompressible isotropic material can be expressed as a general power series[10,11],

$$W = \sum_{i,j=0}^{\infty} c_{ij}(I_1 - 3)^i(I_2 - 3)^j, \tag{4}$$

where the first and second strain invariants are defined in terms of the extension ratios,

$$I_1 = \lambda_1^2 + \lambda_2^2 + \lambda_3^2 \tag{5}$$

and

$$I_2 = \lambda_2^2\lambda_3^2 + \lambda_3^2\lambda_1^2 + \lambda_1^2\lambda_2^2. \tag{6}$$

To second order in the strain, this series expansion gives for a uniaxial extensional strain,

$$W = c_{10}(\lambda^2 + 2\lambda - 3) + c_{01}(\lambda^{-2} + 2\lambda - 3). \tag{7}$$

Differentiation of the strain energy with respect to the principal stretch ratio provides the Mooney–Rivlin relation for the elastic stress, which is written as

$$\sigma_{MR} = v^{-1/3}v_x^{2/3}f(\lambda)\{2C_1 + 2C_2\lambda^{-1}\}, \tag{8}$$

where the C_1 and C_2 are the customary designations for the elastic constants c_{10} and c_{01}. Due to a well-established consonance with at least the strain dependence of the tensile stress in real networks, the Mooney–Rivlin expression is the most often utilized description of the equilibrium tensile behavior of rubbery networks. This agreement with experimental data is, however, limited to tensile deformation, and accordingly Equation (8) is not a valid constitutive equation. Any ability of a model to predict the strain dependence of stress, of course, is not evidence of correct accounting for the crosslink density dependence of stress. Related to this point is the continuing dispute regarding the contribution of trapped topological entanglements to the elastic modulus[12-14].

Real networks are observed, in general, to exhibit elastic behavior that is relatively affine at low strains, while large extension affords greater freedom for spatial fluctuations of the junction points along the stretch direction. Theoretical formulations have been developed which attempt to model the effect on the elastic stress of junction fluctuations and their change with strain. In the constraint theory of Flory, the fluctuation of the junctions is limited to a domain of constraints imposed by steric hindrances from neighboring segments. During network extension, these domains elongate and change their position, effecting a diminution in the damping of junction fluctuations along the principal extension direction. The increase in fluctuations reduces the differential deformation of

network chains and thus the observed modulus. The elastic stress in the constraint model is given by[7,15],

$$\sigma_{con} = (1 - 2/\phi)NkTv^{-1/3}v_x^{2/3}f(\lambda)(1 + f_c/f_p h), \quad (9)$$

where for $\lambda > 1$ the contribution, f_c, to the stress from constraints on junction fluctuations is a decreasing function of strain relative to the phantom network contribution, f_{ph}. This is consistent with the known negative deviation in the elastic stress during extension from the affine model in real networks. In general, the quantity f_c/f_{ph} for a given strain can be obtained by numerical evaluation of free-energy integrals involving functions of the strain[16]. It can be seen by comparison with Equation (9) that the Mooney–Rivlin C_1 is identifiable with NkT and the ratio C_2/C_1 can be taken as a measure of the relative magnitude of the constraints on junction fluctuations. As the deformation proceeds, the reduction in the domain of these constraints effects fluctuations of junctions more like that of a phantom network. A smaller ratio of C_2/C_1 implies less alteration from affine to phantom-like response as the strain increases, either because the junction behavior is relatively unconstrained initially (as in the case, for example, of a network swollen with diluent) or because the severity and spatial domain of the constraints are of a more permanent nature (as exemplified by crosslinks of exceedingly high functionality).

EXPERIMENTAL

The elastomers used in this study were a *cis*-1,4-polyisoprene (SMR-L type *Hevea Brasiliensis*) and a 23.5% styrene, 76.5% butadiene random copolymer (Duradene 706 from the Firestone Tire and Rubber Co.). Crosslinking was done at 160°C for 48 min with dicumyl peroxide as the curative. Five basic network types were prepared:

i. Polyisoprene with 1.0% by weight peroxide, along with 0.05% stabilizer to suppress degradation.

ii. SBR crosslinked neat with respectively 0.05% (SBR05) and 0.10% (SBR10) peroxide.

iii. SBR05 and SBR10 swollen after crosslinking with 33% by volume of nonvolatile paraffin oil. Upon immersion in the paraffin, it is likely that a portion of the soluble fraction of the SBR diffuses out of the specimens. This is a minor effect, however, since the soluble fractions of the SBR rubbers were quite low in both cases. These materials, designated SBR05-S and SBR10-S respectively, were tested in the swollen state. The factor of $v^{-1/3}$ found in equations above for the elastic stress will, according to theory, account for the effect of diluent on the measured elastic properties[8,10].

iv. SBR with 0.2% peroxide crosslinked while in solution with 50% by weight of paraffin oil, the latter and any soluble polymer subsequently extracted with tetrahydrofuran prior to testing. This sample is referred to as SBR-E.

The soluble fraction of all rubbers, f_{sol}, along with the volume fraction of the insoluble network at equilibrium swelling, v_e, are given in Table I. The solvent for the determination of v_e was cyclohexane for the SBR samples and carbon tetrachloride for the NR. The solubility parameter difference between the solvent and polymer is equivalent in these cases [0.3 per $(cal/mL)^{1/2}$ [17]].

TABLE I

RUBBERY NETWORKS EMPLOYED

Sample	ν_x	ν	f_{sol}	ν_r
SBR05	1.0	1.0	.05	0.152
SBR05-S	1.0	0.67	<.05	—
SBR10	1.0	1.0	.11	0.104
SBR10-S	1.0	0.67	<.11	..
SBR-E	0.5	1.0	0[a]	0.0933[a]
NR	1.0	1.0	.04	0.113

[a] All soluble material was extracted prior to testing.

Low network chain densities were used in order to minimize the occurrence of chain scission during mechanical deformation. The maximum molecular extension ratio, λ_x, of a flexible chain can be expressed[18] in terms of the number of main chain bonds, n, and the characteristic ratio, C_n,

$$\lambda_x = (n/C_n)^{1/2} b_p/b, \tag{10}$$

where b is the length of the bond and b_p the projection in the extension direction. Using this relation, the maximum extension ratio at the crosslink densities employed herein is calculated to be over 800%. The present experiments were limited to maximum elongations of 150% or less. Particularly for the higher strain experiments, an absence of significant fracture was demonstrated by confirming reproducibility in the results when the test specimens were reused. Consistent with this, equivalent equilibrium results were obtained with samples in retraction as in extension. The tensile measurements were carried out at room temperature using an Instron 4206, with a Hewlett Packard Model 216 employed for data acquisition and control of the crosshead motion. An initial specimen length of 100 mm was utilized, with a cross-sectional area equal to 19 mm^2. This high specimen aspect ratio minimizes errors associated with clamping effects. For equilibrium experiments, invariance of the stress for 15 min was taken to correspond to elastic equilibrium. Such invariance was typically obtained after a few hours. The stress–strain history for the nonequilibrium experiments consisted of uniaxial extension of the sample at a constant crosshead velocity (the corresponding nominal strain rate, typically 0.08 sec^{-1}, is detailed below). At a given strain level (which was varied in different experiments), the crosshead was instantly reversed, and the sample returned to zero strain at the same velocity. The slight lag in the reversal of the crosshead was measured with a spring employed as the test specimen. The strain history was corrected for this small error.

RESULTS AND DISCUSSION

ELASTIC BEHAVIOR

The equilibrium mechanical response measured for the various materials when subjected to tensile deformation are displayed in Figures 1 through 5.

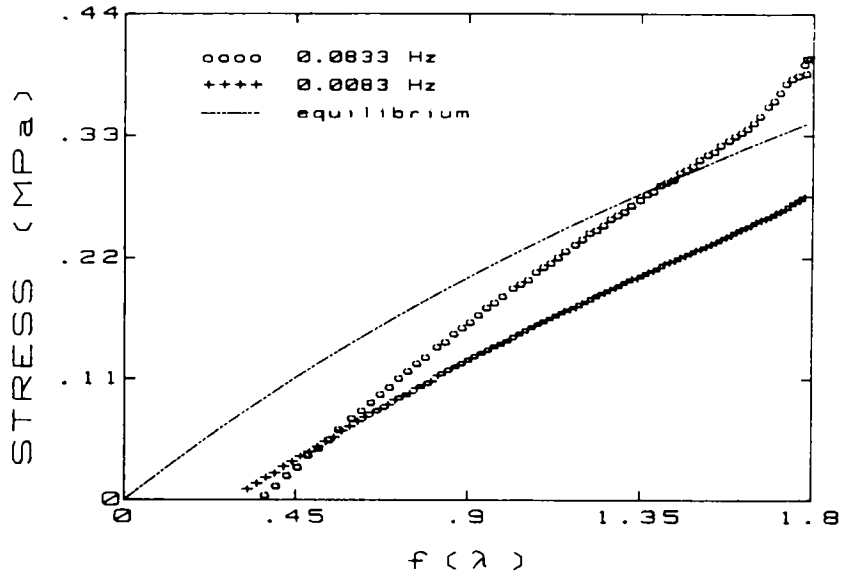

FIG. 1.—The stresses measured for SBR05 during retraction at the indicated nominal elongation rates, after a maximum elongation of 104%. The corresponding values obtained at elastic equilibrium are also indicated.

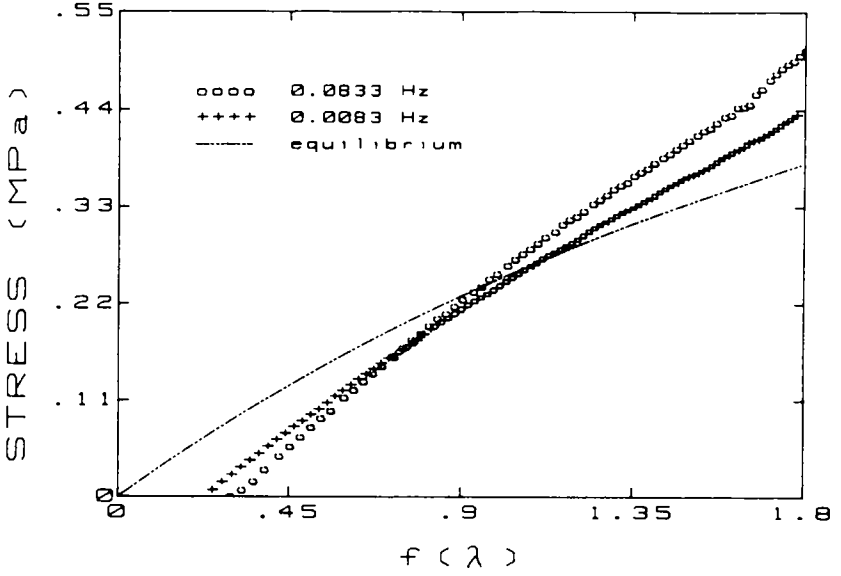

FIG. 2.—The stresses measured for SBR10 during retraction (after staining to a maximum extension ratio of 2.05) at the indicated nominal elongation rates, along with the corresponding values obtained at elastic equilibrium.

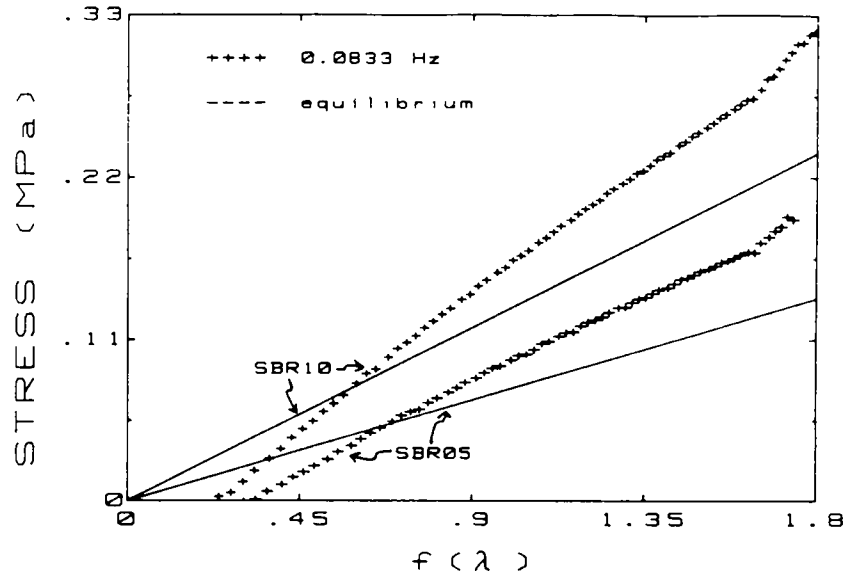

FIG. 3.—The stress at equilibrium and during retraction measured for the SBR05-S and the SBR10-S after extension to $\lambda = 2.0$. The nominal extensional rate was 0.0833 sec^{-1}.

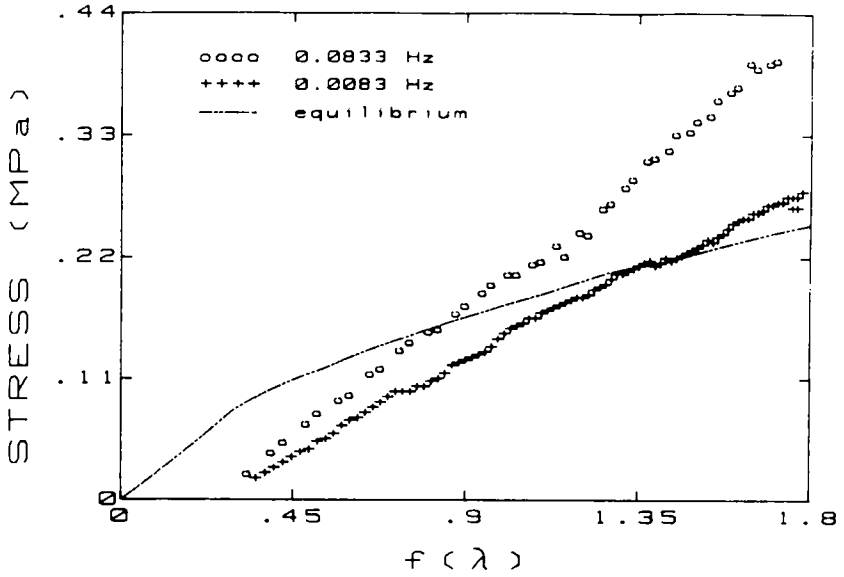

FIG. 4.—The stresses measured for SBR-E during retraction at the indicated nominal elongation rates, subsequent to straining to $\lambda = 2.09$. The corresponding values obtained at elastic equilibrium are indicated.

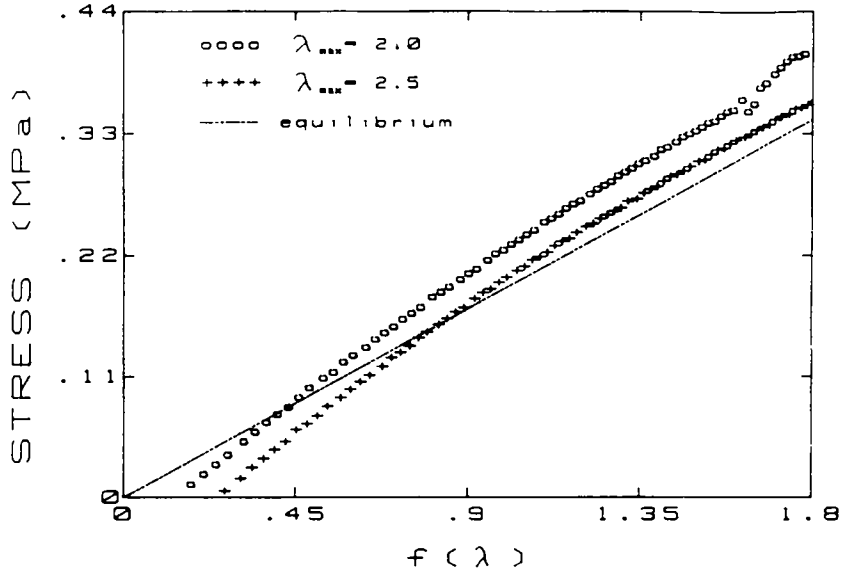

FIG. 5.—The stresses measured for NR during retraction from the indicated extensions, along with the corresponding values obtained at elastic equilibrium. The deformation rate was 0.0833 sec^{-1}.

With two exceptions, the strain dependence of the equilibrium stress for the networks conforms to the Mooney–Rivlin description [Equation (8)] over the range of strains employed. The polyisoprene rubber at very high extension ratios exhibits a decreasing stress due to the onset of strain-induced crystallization. It is a thermodynamic requirement that crystallization effected by the application of load must at equilibrium reduce the load. This orientational crystallization requires high elongation (>450%), however, and over the deformation range of interest herein, the strain dependence of the elastic stress is well described by Equation (8). The behavior of the SBR-E material also deviates from the Mooney–Rivlin relation, but the divergence is only seen at the lowest extensions. The SBR-E was in solution during crosslinking, giving rise to an initially swollen network. Upon removal of the diluent, the network chains assume a more compact configuration. Extension of this "collapsed" network will bring the chain configurations closer to their unperturbed state; that is, the initial stages of extension are on a microscopic level akin to the removal of compressive loading. The Mooney–Rivlin expression is not a valid constitutive equation due to its failure to accurately describe the material response to all types of strain. In particular, deformations in which the stretch ratio goes from less than to greater than unity are poorly described by Equation (8)[16,19]. The initial nonlinearity in the data in Figure 4 reflects this effect. The values obtained for the elastic constants, C_1 and C_2, for the higher strains, along with the results for all the rubbers, are listed in Table II.

Based on the measured v_e, crosslink densities were calculated for the various rubbers assuming a perfect network using

TABLE II

EQUILIBRIUM RESULTS[a]

Sample	$N \times 10^4$ (mL^{-1})	C_1	C_2	C_2/C_1	$N_{app} \times 10^4$ (mL^{-1})
SBR05	1.1	.064	.156	2.4	0.62
SBR05-S	1.1	.055	.072	1.3	0.28
SBR10	2.2	.114	.197	1.7	0.88
SBR10-S	2.2	.101	.108	1.1	0.67
SBR-E	1.5	.032[b]	.113[b]	3.5	0.75
NR	1.4	.112	.168	1.5	1.19

[a] N was determined from v_e using Equation (11), while the apparent crosslink density, N_{app}, was obtained from application of Equation (1) to the 0.083 sec^{-1} retraction data at $\lambda = 1.3$ in Figures 1 through 5.

[b] For $\lambda > 1.3$ only.

$$\ln (1 - v_e) + v_e + \chi v_e^2 = -NV_s v_r (v_e^{1/3}). \tag{11}$$

The polymer–solvent interaction parameter is defined as

$$\chi = V_p/\mathrm{RT}(\Delta\delta)^2, \tag{12}$$

where $\Delta\delta$ represents the solubility parameter difference between the polymer and the solvent, and V_p and V_s are their respective molar volumes. As has been experimentally corroborated[20], the assumption of phantomlike behavior embodied in Equation (11) is not inappropriate for networks in the equilibrium state of swelling. From these results, displayed in Table II, it is seen that reduction by a factor of two of the peroxide level in the SBR produces a proportional decrease in crosslink density (the data for SBR05 and SBR10). The corresponding reduction in the elastic constant C_1 by 56% is of the expected magnitude if this quantity reflects principally the abundance of covalent crosslinks. After swelling in paraffin, the two SBR samples exhibit slightly reduced values for C_1. If C_1 represents only the concentration of network chains, its value is not expected to change upon their swelling. Although, since swelling facilitates the attainment of equilibrium, this slight decrease could reflect incomplete relaxation in elastic measurements on the dry networks, it has similarly been reported elsewhere that the reduction in modulus due to swelling exceeds the predicted $v_e^{1/3}$ decrement[8], suggesting that the diluent effect is being underestimated. In the derivation of the factor of $v_e^{1/3}$ to account for the presence of diluent, an elastic energy directly proportional to strain and strictly affine junction motion were assumed[10]. In fact, the increasing Brownian motion of the junctions upon their dilution, effecting a more nonaffine response, must contribute further to the reduction in the modulus of swollen rubbers[21], in qualitative agreement with the present experimental results.

While for either dry or swollen SBR samples, C_1 increases in proportion to increases in crosslink density, the ratio C_2/C_1 varies in inverse fashion with the concentration of crosslinks. The reduction in the strain dependence of the elastic modulus reflects firmer embeddment of junctions at higher crosslinking levels, whereby the domain of constraints on junction motions is less affected

by strain. As inferred from either equilibrium swelling or mechanical measurements, the SBR10 has the highest crosslink density of all samples, and accordingly it is expected to exhibit the most nearly affine deformation behavior. Since the interpenetration of chains is less for shorter networks chains, the severity of constraints is less influenced by straining. The SBR10 has, accordingly, the lowest C_2/C_1 ratio of any of the dry SBR elastomers.

Dilution serves to isolate to some extent the crosslink sites from restrictions from surrounding network chains. This implies a smaller value of C_2/C_1 than in the absence of diluent, since, whereas in the latter situation the severity of constraints on junction motion becomes reduced at higher extensions, swollen networks are relatively unconstrained initially resulting in a more strain-independent elastic modulus. The SBR05-S, having a low density of chemical crosslinks which are, moreover, in the presence of diluent, represents the network of most phantomlike behavior. The enhanced junction mobility results, for example, in an elastic stress at $\lambda = 1.1$ for the SBR05-S that is 59% of that of the corresponding network in the unswollen condition (SBR05). Since the damping of junction fluctuations is diminished at higher strains, differences between swollen and dry networks of the same crosslink concentration become minimized. This reduced effectiveness of topological constraints is seen in the elastic stress at $\lambda = 5.0$, which for the SBR05-S is now within 73% of that of the SBR05. The elastic response of the SBR10 and of the SBR10-S similarly become more nearly equivalent at higher extensions.

The solution crosslinked rubber (SBR-E for which $v_x = 0.5$) had a crosslink density that was intermediate between that of the SRB10 and the SBR05 according to Equation (11). The obtained C_2/C_1 ratio was significantly higher than for the latter, an unexpected result in light of previous reports[22,23]. The reduction in steric restrictions on the network strands which presumably results from crosslinking in solution should reduce the relative value of C_2. As noted above, however, the stress–strain data for SBR-E did not conform to Equation (8) at extension ratios less than about 1.3. The initial state of compression of the network chains, brought about by removal of the diluent present during crosslinking, invalidates the Mooney–Rivlin approach to the SBR-E data. Interpretation of the significance of the fitting parameters in terms of the network topology is consequently ill advised.

The functionality of NR junctions formed using peroxide is expected to be four[24,25]. These tetrafunctional crosslinks are relatively freer than the junction structure in the SBR rubbers, in which free-radical crosslinking is accompanied by some chain reaction and consequent higher functionality[24,25]. This differing reactivity required the use of a significantly higher concentration of peroxide in the NR in order to achieve a crosslink concentration comparable to that of the SBR rubbers. Although its crosslink density (as measured by v_e) is intermediate between that of the SBR10 and SBR05, the ratio of C_2/C_1 is lower for the NR than for either of the neat SBR samples. The more unconstrained Brownian motion of the lower functionality crosslinkages facilitates their rearrangement to better accommodate the imposed deformation. The C_2/C_1 ratio, which reflects alteration in constraints on the network with strain, is consequently smaller.

To summarize, it is seen that the degree of strain independence in the elastic response is a reflection of network architecture. Networks with a low concentration of low functionality junctions (sample NR) or in the presence of diluent (SBR05-S and SBR10-S), have the most strain-independent elastic modulus, since, at the low crosslink concentrations employed herein, their junctions are relatively uninhibited, even at low strain. Networks with more extensively constrained junctions have a large C_2/C_1 ratio only to the extent the domain of the constraints can be reduced by elongation (*e.g.*, SBR-05 and SBR-E). The most nearly affine network, SBR-10, has an intermediate ratio of C_2/C_1,, since constraints arising from its higher concentration of crosslinks of higher functionality are less effectively ameliorated by deformation; thus, it exhibits a response that becomes less phantomlike at higher elongations. In general, deviations in the equilibrium modulus with strain are an indication, not of affine or of nonaffine motion, but rather a change in the degree of affineness of the mechanical response.

TENSILE RETRACTION RESULTS

The stresses developing in the various networks during uniaxial extension and retraction were measured at various deformation rates. The stresses during retraction are, of course, equivalent to those during extension only when the reciprocal of the rate of straining greatly exceeds the longest relaxation time of the material, at least in the absence of rupture of network chains. The latter is difficult to realize under elastic equilibrium conditions, even when the maximum strain does not exceed the level corresponding to complete extension of any network strands. Since reptative chain motions are largely suppressed, attainment of mechanical equilibrium typically requires at least a few thousand minutes; consequently, the duration of a reversible deformation experiment can extend over several days. Maintaining an elastomer in a strained state, even one that is below the critical strain associated with catastrophic fracture, will nevertheless enhance bond rupture by the strain-induced reduction of the activation energy for the rupture[26,27]. It has been observed that the execution of strain cycles at rates sufficiently slow such that elastic equilibrium conditions prevailed was accompanied by the development of pervasive whitening of the test specimens[28]. While this is a clear indication of chain rupture, the stresses during retraction of damaged networks are nevertheless found to be equivalent in magnitude to the extensional stresses. The broken bonds are the result of ozone-induced microcracking and thus are localized at the surface of the sample. While of sufficient size and abundance to effect noticeable optical scattering, they are nonetheless insignificant with respect to the precision of the stress measurements[28].

Of interest herein with regard to tensile retraction experiments are the recent reports describing an apparent conformation of the retractive response of rubbers to mathematical formulations appropriate for equilibrium mechanical behavior[2-6]. In particular, it has been found that the stress during retraction is often directly proportional to the strain function defined according to Equation (2). Since this function is a result of the statistical theories of rubber elasticity,

such proportionality has suggested to some investigators that tensile retraction experiments conducted at relatively high deformation rates may reveal equilibrium properties of a network, ostensibly obviating any need for the time-consuming acquisition of actual equilibrium mechanical data. The implication is that the topology of the network chains is altered by strain reversal, and mechanical behavior mimicking that of a phantom network will prevail. While the seemingly dubious nature of such claims invites their casual dismissal, the continued occurrence of experimental data suggestive of a direct relationship between the retraction response of rubbers and their elastic behavior warrants more serious scrutiny. To determine whether any fundamental connection exists in this regard it is necessary to ascertain:

i. if the proposed linearity is universally maintained among networks of various architecture,

ii. whether the stresses during retraction are in fact independent both of the reversal strain and of the deformation rate, and

iii. if the crosslink density deduced by this procedure is correct.

The stresses after uniaxial extension to various elongations were measured for the rubbers. Displayed in Figures 6 through 9 are comparisons of the stresses measured at an extension ratio equal to 1.3 at equilibrium, during extension, and during retraction from different maximum strains. These results, representative of the trends observed through most of the retraction cycle, demonstrate that the stresses during retraction are a decreasing function of the maximum strain. As would be expected, the faster-relaxing networks exhibit the smallest

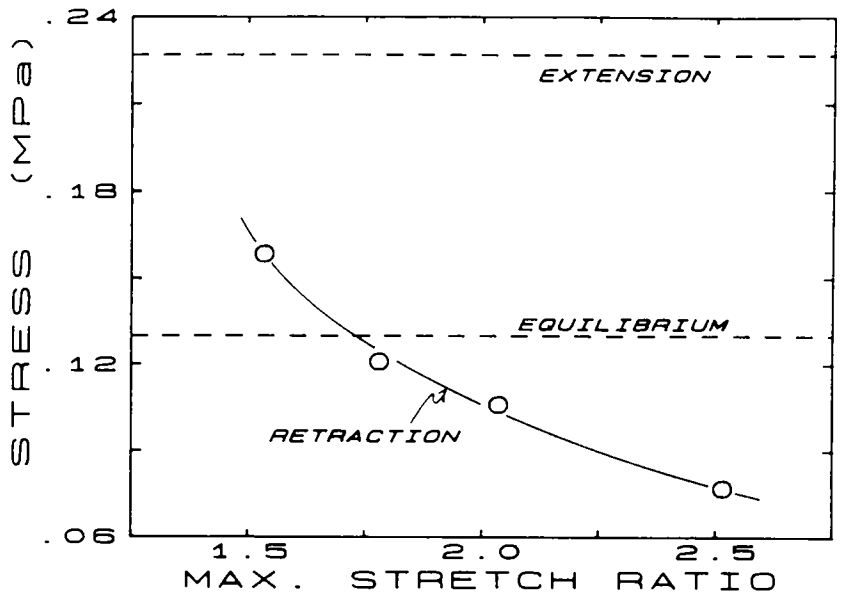

FIG. 6.—The stress measured at an extension ratio equal to 1.3 for the SBR05 during its return from uniaxial extension of various magnitudes. The equilibrium and extensional stresses for the same strain are indicated by the horizontal dashed lines.

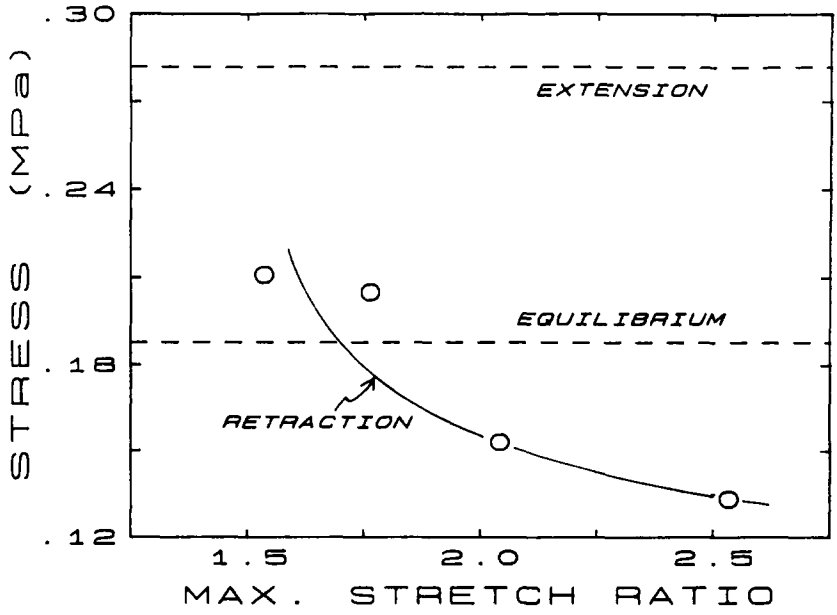

FIG. 7.—Comparison for SBR10 of the magnitude of the stresses measured at $\lambda = 1.3$ during retraction from various maximum extensions with the corresponding stress at the same strain during extension and at equilibrium.

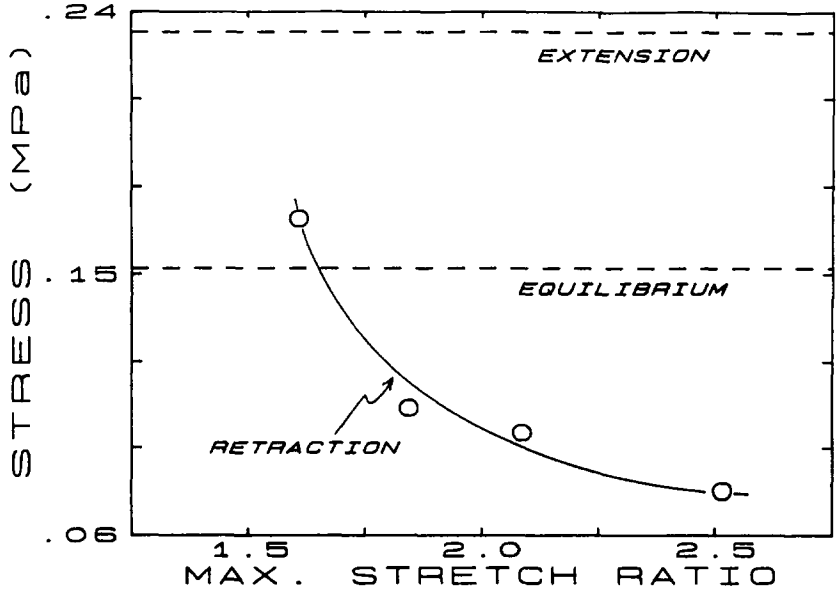

FIG. 8.—The retraction stress for SBR-E at $\lambda = 1.3$ in comparison to the equilibrium and extensional stresses for the same strain.

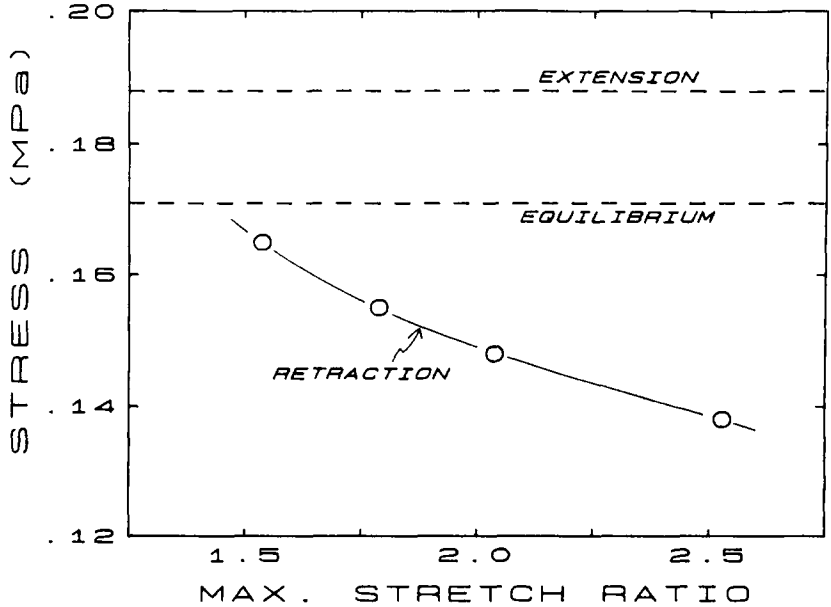

FIG. 9.—The retraction stress for NR at $\lambda = 1.3$ in comparison to the equilibrium and extensional stresses for the same strain.

difference between stresses during extension and at equilibrium. Related to their relaxation behavior[1], these same networks have the smallest stresses during retraction relative to the stress at equilibrium. Particularly at higher reversal strains, this can result in stresses at a given retractive strain that are less than the corresponding elastic stress. This indicates that some portion of the network structure is under compression, even though the bulk specimen is still elongated. Obviously stress–strain behavior reflective of the extent of stress relaxation in the material can not directly bear upon the equilibrium mechanical properties. This dependence of the stresses on the reversal strain has previously been noted, notwithstanding the inferences nevertheless made therein regarding equilibrium network properties[3]. Depending on the maximum extension, the stress at a given retractive strain may be found to be equivalent to the corresponding equilibrium value; however, the particular conditions for this correspondence vary with the rubber structure. This is not a general feature of retraction data.

Displayed in Figures 1 through 5 are the stresses measured for the various rubbers upon tensile retraction (from a maximum extension of 100% unless noted otherwise). At a deformation rate (defined by the ratio of the extensional velocity to the initial length) of 0.083 sec^{-1}, proportionality between the retraction stress and the $f(\lambda)$ of Equation (2) is most closely approximated in the diluted networks (SBR05-S and SBR10-S) and in the NR. A unifying factor therein is that these are the rubbers which exhibit elastic behavior most nearly in accordance with that of a phantom network, as discussed above, and which are

possessed of the most rapid stress-relaxation behavior[1]. The better agreement with the form of Equations (1) and (3) evident in the retraction stresses than those measured during extension is probably associated with the compressive contributions to the total stress. These serve to compensate for neglect [in Equation (1)] of the C_2 term by introducing a time dependence in the viscous response that mimics to some extent the strain dependence of the elastic response. Thus, while conformance of nonequilibrium deformation behavior to the strain dependence given by elastic expressions such as Equations (1) and (3) may ostensibly be realized, it appears to be associated with those rubbers that have an elastic modulus only weakly strain dependent and in which viscoelastic effects are most rapidly dissipated. Note also that while at deformation rates an order of magnitude slower, the retraction data for the SBR05 and SBR10 networks appear more linear when plotted in this manner than the data obtained at 0.083 sec^{-1}, such rate dependence of the mechanical response during retraction belies various claims that following an initial loading, tensile experiments become representative of equilibrium[4-6]. Moreover, even when retraction stresses exhibit proportionality to $f(\lambda)$, the ratio of these quantities is not the NkT of the elastic theories. This can be seen, for example, in the comparison (Table II) of the N determined by swelling to the apparent crosslink density inferred from the use of the retraction stresses in Equation (1). Even the rank ordering of network crosslink densities is not predictable from these stresses, since they are determined as much by the relaxation behavior as by the network structure *per se*. Addition of diluent reduces the apparent crosslink density obtained from Equation (1) since the retraction stresses are closer to their equilibrium value, and thus the error arising from neglect of the C_2 term is not compensated for as fortuitously. Although for a series of rubbers differing only in crosslink density, the magnitude of the retraction stresses will reflect the concentration of network chains, this statement is equally valid for stresses measured during extension.

The strain during retraction at which the stress becomes equal to zero is commonly referred to as the "set," or more misleading, the "permanent set." This irrecovered strain is indicative of compressive strains in the material. Negative loads *per se* are usually not measured, since the high aspect ratio of tensile specimens give rise to buckling and consequently very low compressive forces; however, even at precisely zero stress, the macroscopic strain can be nonzero due to the distribution of network chain lengths. The contribution to the total stress from a network chain is proportional to the displacement of the chain, relative to its equilibrium mean square end-to-end separation. A shorter network chain will consequently contribute more strongly to the stress than a longer chain having the same absolute displacement. A distribution in the lengths of network chains can thus give rise to a strain that is nonzero at the moment the stress becomes zero. The network is not at equilibrium, however, and will continue to deform (*i.e.*, recover its initial dimensions) in the absence of external load. The influence of network compression can be inferred from Figure 10, in which the strain measured at zero load is seen to correlate with the difference between the stress during retraction and the elastic stress at equivalent strains. This set is not permanent, although complete recovery, involving diffusion of branched chain ends, may be a very slow process.

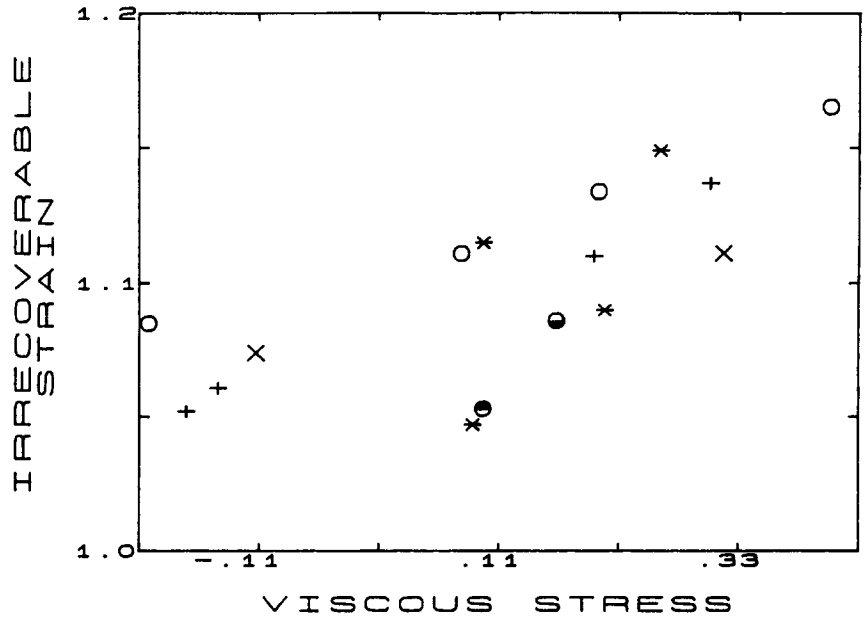

FIG. 10.—The instantaneous set (that is, the extension ratio at which the load goes to zero during retraction) measured for the rubber samples (○ SBR-5, + SBR10, ◒ SBR05-S, ◓ SBR10-S, * NR, and × SBR-E) *versus* the normalized viscous stress. The latter is the difference between the retractive stress at $\lambda = 1.3$ and the elastic stress at the same strain, divided by the elastic stress. The measurements were made during return from maximum extensions of from $\lambda = 1.5$ to 2.5.

SUMMARY

The elastic response of rubber has a direct and controllable dependence on structure. The behavior of the various networks described herein is seen to be consonant with the well-established roles of spatial fluctuations of crosslinks and the inhibition of this Brownian motion by steric and entanglement constraints from neighboring chains. Although elasticity also governs to a large extent the nonequilibrium mechanical response, interpretation of the latter in terms of network structure is obscured by viscoelasticity. The junctions of real networks, having some freedom to reconfigure themselves away from strictly affine displacement, exhibit lower equilibrium stresses than predicted by the statistical model for affine chains. To the extent that this overestimation of the model and the compressive component of the retraction response mimic the effect of departures from equilibrium, some conformance of network behavior during retraction to Equation (1) may be realized. It is such a fortuitous circumstance that likely underlies the various proposals commending such a relationship. A measure of junction density is generally not obtainable from deformation experiments in which dissipative processes are active.

ACKNOWLEDGMENT

Supported in part under Naval Research Contract No. N0001488WX24207.

REFERENCES

[1] C. M. Roland, RUBBER CHEM. TECHNOL. **62,** 880 (1989).
[2] R. F. Fedors, *NASA Tech. Brief* **7**(2), 1 (1982).
[3] R. A. Hayes, RUBBER CHEM. TECHNOL. **59,** 138 (1986).
[4] W. L. Hergenrother, *J. Appl. Polym. Sci.* **32,** 3039 (1986).
[5] W. L. Hergenrother, *J. Appl. Polym. Sci.* **32,** 3683 (1986).
[6] Y.-H. Zang, R. Muller, and D. Froelich, *J. Rheol.* **30,** 1163 (1986).
[7] P. J. Flory, *Polym. J.* **17,** 1 (1985).
[8] L. R. G. Treloar, *Rep. Prog. Phys.* **36,** 755 (1973).
[9] J. E. Mark, *J. Am. Chem. Soc.* **92,** 7252 (1970).
[10] L. R. G. Treloar, "The Physics of Rubber Elasticity," Clarendon, Oxford, 1975.
[11] R. S. Rivlin in "Rheology," F. R. Eirich, Ed., Academic Press, New York, 1956, ch. 10.
[12] J. D. Ferry, "Viscoelastic Properties of Polymers," Wiley, New York, 1980.
[13] B. Erman and P. J. Flory, *Macromolecules* **15,** 806 (1982).
[14] A. Duabult, B. Deloche, and J. Herz, *Macromolecules* **20,** 2096 (1987).
[15] P. J. Flory and B. Erman, *Macromolecules* **15,** 800 (1982).
[16] B. Erman and P. J. Flory, *J. Chem. Phys.* **68,** 5363 (1978).
[17] "Polymer Handbook," J. Brandup and E. H. Immergut, Eds., Wiley, New York, 1966.
[18] P. Smith, R. R. Matheson, and P. A. Irvine, *Polym. Commun.* **25,** 294 (1984).
[19] H. Pak and P. J. Flory, *J. Polym. Sci., Polym. Phys. Ed.* **17,** 1845 (1979).
[20] J.-P. Queslel, F. Fontaine, and L. Monnerie, *Polymer* **29,** 1086 (1988).
[21] P. J. Flory, *Macromolecules* **12,** 119 (1979).
[22] B. Erman and J. E. Mark, *Macromolecules* **20,** 2892 (1987).
[23] R. F. Boyer and R. L. Miller, *Polymer* **28,** 399 (1987).
[24] A. Y. Coran in "Science and Technology of Rubber," F. R. Eirich, Ed., Academic Press, New York, 1978, ch. 7.
[25] G. G. A. Bohm and J. O. Tveekrem, RUBBER CHEM. TECHNOL. **55,** 575 (1982).
[26] C. M. Roland and C. R. Smith, RUBBER CHEM. TECHNOL. **58,** 806 (1985).
[27] V. S. Kuksenko and V. P. Tamuzs, "Fracture Micromechanics of Polymer Materials," Martinus Nijhoff, The Hague, 1981.
[28] C. M. Roland and W. J. Sobieski, RUBBER CHEM. TECHNOL. **62,** 683 (1989).